JOURNAL OF OPTOELECTRONICS AND ADVANCED MATERIALS Vol. 12, No. 5, May 2010, p. 1213 - 1219

Synthesis and characterization of acrylic bone cements reinforced with hydroxyapatite

J. SIMITZIS*, D. E. BACIU, S. SOULIS, M. TZEDAKI
National Technical University of Athens, School of Chemical Engineering, Department III "Materials Science and Engineering", Laboratory Unit "Advanced and Composite Materials", 9 Heroon Polytechniou str., Zografou Campus, 157 73 Athens, Greece

---

Acrylic bone cements based on poly (methyl methacrylate) (PMMA) reinforced with hydroxyapatite (HA) were synthesized by polymerization of MMA with PMMA prepolymer. The materials were characterized by Fourier transform infrared spectroscopy (FTIR), X-ray diffraction (XRD), nuclear magnetic resonance spectroscopy (NMR) and scanning electron microscopy (SEM) and the molecular weight was viscosimetrically determined. The molecular weight of PMMA bone cement without HA is about twice that of the initial PMMA. Acrylic bone cements reinforced with HA can be an advantageous solution for problems of bone filling as well as bone regeneration.

(Received March 11, 2010; accepted May 26, 2010)

Keywords: acrylic bone cements, hydroxyapatite, FTIR, XRD, NMR, SEM

---

1. Introduction

Acrylic bone cements of poly (methyl methacrylate), (PMMA) have been widely used in orthopaedic surgery for anchoring prostheses in total hip or knee replacements for several decades [1]. The clinical use of this type of bone cement is accompanied by several complications due to its limited mechanical properties and poor compatibility with bone. The material is brittle and does not adhere to bone to induce bone formation. In addition, the exothermic during the polymerization lead to a damage of bone tissue [2]. Several investigators have been researching alternative formulations to improve the deficiencies above noted. Furthermore, bioactive bone cements including calcium phosphate cements and polymeric cements with bioactive fillers have been reported as alternatives to the common acrylic bone cements. The choice to include a bioactive additive in combination with the acrylic polymer is attractive due to its bone bonding ability and its contribution to more appropriate properties of the composite [3].

Hydroxyapatite, $Ca_{10}(PO_4)_6(OH)_2$ (HA) material has been clinically applied in many areas of dentistry and orthopaedics because of its excellent osteoconductive and bioactive properties which is due to its chemical similarity with the mineral component of hard tissues (e.g. bone) [4]. However, fragility and poor mechanical properties of sintered HA ceramics limit their application as artificial implants [5]. Hydroxyapatite (HA) as filler in composites reinforces the polymer, especially by increasing its stiffness, and improving bone bonding properties of the materials. The latter is essential to achieve early bone in-growth and fixation of implants by bone tissues. It has been found the addition of a certain amount of hydroxyapatite to the polymer matrix may alternate a non-bioactive polymer into a bone-bonding composite [6].

The aim of this work is the synthesis of acrylic bone cements reinforced with crystalline HA, by bulk polymerization of MMA in the presence of PMMA used as prepolymer and the characterization of the products. The Fourier transform infrared spectroscopy (FTIR), the X-ray diffraction (XRD), the nuclear magnetic resonance spectroscopy (NMR), and the scanning electron microscopy (SEM) will be used to characterize the materials, whereas the molecular weight of the prepolymer PMMA and the acrylic bone cement will be viscosimetrically determined.

2. Experimental

2.1. Preparation of PMMA beads

PMMA beads were prepared by free radical suspension polymerization. The raw materials: water, suspending agent (CMC) (Fluka), monomer (MMA) (Fluka) and initiator (BPO) (Merck) were added in a 1L three-necked reactor equipped with a reflux condenser, a mechanical stirrer and a temperature control system. Specifically, 600 ml of water was added into the reactor and then 1.2g of carboxy methyl cellulose (CMC) as suspending agent was dissolved. The monomer of methyl methacrylate (MMA) was repeatedly washed with 5% (w/v) NaOH / aq. solution and with distilled water in order to remove the inhibitor containing in the MMA. The monomer phase was prepared by dissolving of 0.6 g of benzoyl peroxide (BPO) as initiator in 60 ml MMA and added into the reactor using a dropping funnel after the temperature of the aq. solution of CMC was reached 70 ^{0}C. The polymerization took place at 75 ^{0}C for 2h and then at 80 ^{0}C for 1h under strong stirring with 600 rpm, in order to maintain the organic phase in suspension. The polymerization was stopped by the addition of cold water into the reactor. The polymer was isolated by precipitation with 200 ml methanol under stirring for 15 minutes. The polymer beads were washed several times with distilled water, sieved and dried at 60 ^{0}C for 24 h and was used as prepolymer in the next procedure concerning the synthesis of acrylic bone cement.

2.2. Preparation of sintered HA powder

The sintered HA powder was produced by the sol-gel method [7] as follows:

A defined amount of phosphoric pentoxide (P_2O_5) was dissolved in absolute ethanol to form a 0.5 mol/l solution. A defined amount of calcium nitrate tetrahydrate ($Ca(NO_3)_2 \cdot 4H_2O$) was also dissolved in absolute ethanol to form a 1.67 mol/l solution. Both solutions were mixed in a molar ratio of Ca/P = 1.67. The mixture was continuously stirred for about 24 h at room temperature. Then, the gel formed, was dried at 80 °C for 24 h in an electrical air oven. The dried gels were ground and sintered up to 600 °C for 6 h in an electrical furnace under air atmosphere with a heating rate of 10 °C/min.

2.3. Preparation of acrylic bone cements reinforced or not with sintered HA powder

A solution of PMMA beads in MMA containing benzoyl peroxide (BPO), as free radical initiator (0.5 % w/v of MMA) was polymerized in the presence of sintered HA powder or not. The components of bone cement composite were hand-mixed for ca. 5 min until the mixture became a paste of high viscosity. Then, the paste was placed into small parallelepiped molds with dimensions of 50x8x4 mm and the polymerization took place at 60 ^{0}C for 24 hours to give acrylic bone cement or acrylic bone cement reinforced with HA powder in 13 % w/w.

The PMMA prepolymer was characterized by FTIR, XRD, NMR and SEM and its molecular weight was viscosimetrically determined. The structure of the HA powder sintered up to 600 ^{0}C for 6 h was characterized by FTIR, XRD, NMR and SEM. The acrylic bone cement reinforced with HA or not was characterized by FTIR, XRD, NMR and SEM and its molecular weight was viscosimetrically determined.

FTIR spectra were recorded using a Perkin Elmer Spectrum 2000, on discs prepared by mixing of the sample powder with KBr.

XRD measurements were performed with a Siemens D5000 X-Ray Diffractometer by using sample of the material as powder.

^{1}H- NMR spectra of the sample in $CDCl_3$ were recorded on Bruker DPX-300 spectrometer operating at 300 MHz.

The SEM-EDS studies were carried out in a FEI Quanta 200 Scanning Electron Microscope (SEM).

According to the viscosimetric method, the viscosity of the pure solvent (toluene) and the polymer solution (PMMA/toluene) at concentration of 0.1, 02, and 0.4 % (w/v) at 30 ^{0}C was determined, using an Ubbelohde type viscometer and then the molecular weight of the polymer was calculated.

3. Results and discussion

3.1. PMMA beads

The FTIR spectrum of the PMMA prepolymer is shown in Fig.1.

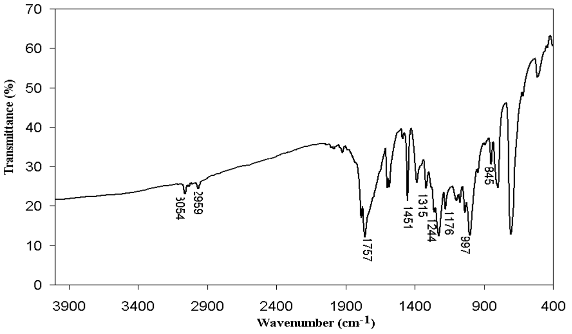

Fig.1. FTIR spectrum of PMMA beads

According to literature, the characteristic vibration bands of PMMA appear at 1757 cm^{-1} ν(C=O) and 1451 cm^{-1} ν(C–O). The bands at 3054 and 2959 cm^{-1} correspond to the C–H stretching of the methyl group (CH3) and the bands at 1315 and 1451 cm^{-1} are associated with C–H symmetric and asymmetric stretching modes, respectively. The 1244 cm^{-1} band is assigned to torsion of the methylene group (CH2) and the 1176 cm^{-1} band corresponds to vibration of the ester group C–O, while C–C stretching bands are at 997 and 845 cm^{-1} [8, 9, 10].

The XRD diffractogram of PMMA beads is shown in Fig. 2.

PMMA is known to be an amorphous polymer and shows three broad peaks at 2Θ values of 11.62 ^{0}, 30.67 ^{0} and 31.96 ^{0} (d spacing aprox. 7.61, 2.91 and 2.79Å correspondingly) with decreasing intensity. According to literature, the shape of the first most intense peak reflects the ordered packing of polymer chains while the second peak denotes the ordering inside the main chains [8].

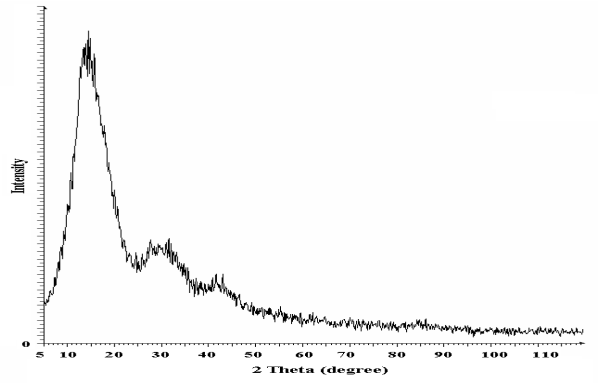

Fig. 2. XRD diffractogram of PMMA beads.

SEM images of PMMA beads prepared by suspension polymerization are shown in Fig. 3 (a, b). As clearly seen, the PMMA beads have spherical form with diameter between 17 and 250 μm determined both from SEM images and proper sieves. The shape and the size of the beads depend on the suspended MMA as droplets into the water by a proper mixing rate during the polymerization.

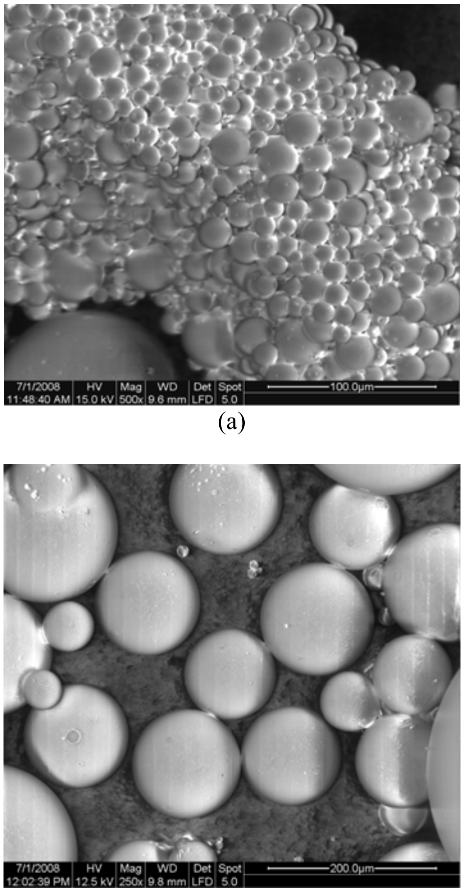

(a)

(b)

Fig. 3. SEM images of PMMA beads: (a) magnification 800x; (b) magnification 250x.

According to Fig. 4, the limiting viscosity number of PMMA beads is calculated as [n] = 0.4189 (100ml/g). The corresponding molecular weight is calculated from the Mark-Houwink-Sakurada equation:

$$[n] = K\,M^{a},$$

where M is the molecular weight of the polymer, K and a are two parameters with the following values for the defined system [11]:

$K = 7.0 \times 10^{-3}$ ml/g
$a = 0.71$

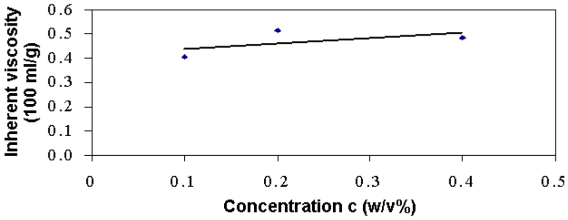

Fig. 4. Plot of inherent viscosity versus the concentration of polymer c.

The molecular weight of PMMA beads was calculated as $\mathbf{M_w = 2x10^5}$.

3.2. Sintered HA powder

The FTIR spectrum of the sintered hydroxyapatite powder at 600 ^{0}C for 6 h is shown in the Fig. 5.

According to the literature, the first indication for the formation of hydroxyapatite is the broad band between 1032 and 1089 cm^{-1} which is attributed to the PO_4^{3-} absorption bands. The bands at 960 cm^{-1} and 568 - 601 cm^{-1} correspond to the symmetric P-O stretching vibration of PO_4^{3-} ion. The bands at 876, 1418 and 1463 cm^{-1} are attributed to the carbonate group (CO_3^{2-}). The characteristic peaks at 3570 cm^{-1} and 630 cm^{-1} are attributed to the stretching modes of hydroxyl groups (OH^-) in the hydroxyapatite [12, 13, 14].

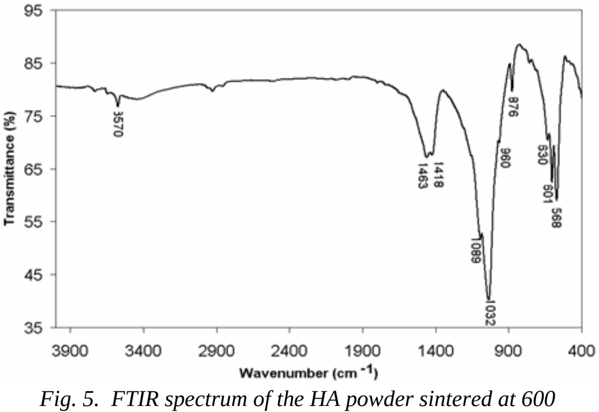

Fig. 5. FTIR spectrum of the HA powder sintered at 600 ^{0}C for 6h.

The XRD diffractogram of sintered HA powder at 600 ^{0}C for 6h is shown in Fig. 6.

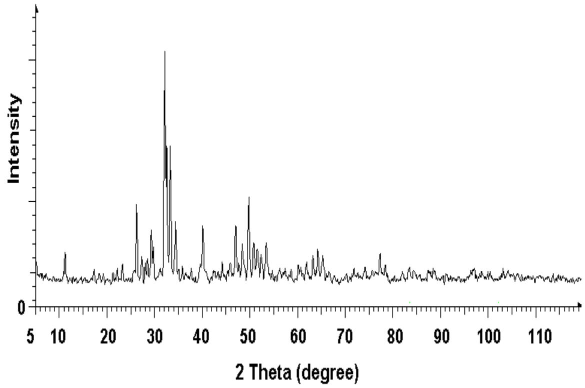

Fig. 6. XRD diffractogram of sintered HA powder.

According to XRD, the sintered hydroxyapatite powder shows peaks with high intensity which belongs to the crystalline hydroxyapatite and peaks of low intensity attributed to b-tricalcium phosphate (TCP) and CaO derived from a small decomposition of HA powder [7, 15]. According to the diffraction peaks, the corresponding d spacings (Å) were determined: 3.43 (2Θ=25.8 ^{0}), 3.08 (2Θ=28.9 ^{0}), 2.81 (2Θ=31.7 ^{0}), 2.62 (2Θ=34.0 ^{0}), 2.25 (2Θ=39.9 ^{0}), 1.94 (2Θ=46.7 ^{0}), 1.88 (2Θ=48.1 ^{0}), 1.84 (2Θ=49.4 ^{0}) and 1.71 (2Θ=53.2 ^{0}). These d spacings are very close to those filed in JCPDS card no. 09-432 for HA crystallized in the hexagonal system [4]. Furthermore, the above results (XRD diffractogram and d spacings) are comparable with those of HA presented in literature [7, 15].

According to SEM images presented in Fig. 7, the morphology of the final sintered HA has porous structure with agglomerated particles.

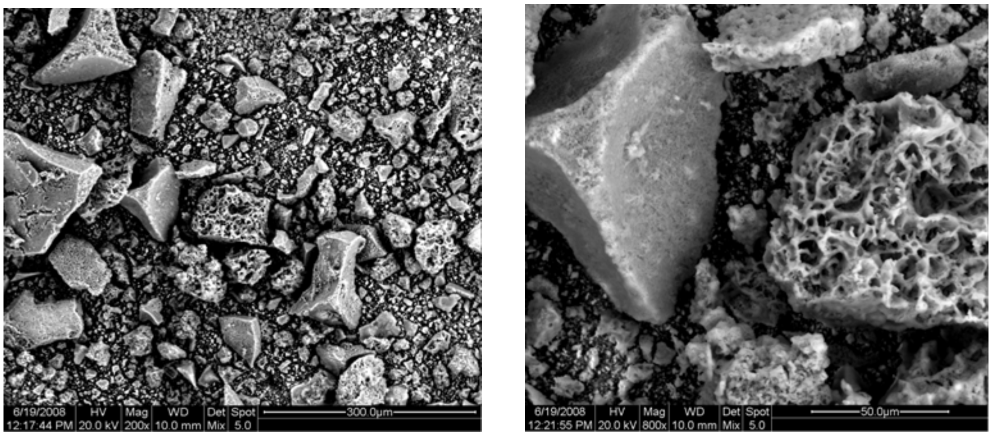

(a) (b)

Fig. 7 SEM images of sintered HA powder: (a) magnification 200x; (b) magnification 800x.

3.3 Acrylic bone cement reinforced or not with HA

Fig. 8 shows the FTIR spectra of both acrylic bone cements reinforced with sintered HA powder or not.

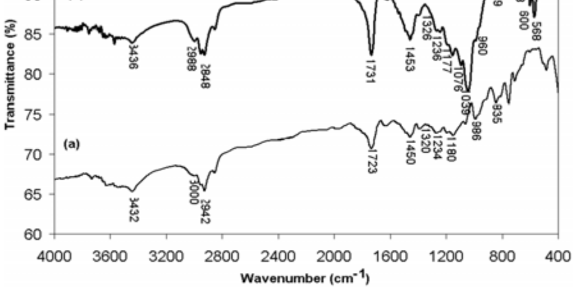

Fig.8. FTIR spectra of (a) acrylic bone cement without HA and (b) reinforced with sintered HA powder.

All the characteristic vibration bands of PMMA. are presented, Fig. 8 (a), and the main characteristic vibration bands of PMMA appear at 1757 cm^{-1} (C=O) and in the fingerprint at 1451 cm^{-1} (C–O) [8, 9, 10].

The presence of HA powder in the acrylic bone cements is indicated by the additional vibration bands corresponding to HA powder, as shown in Fig. 8 (b). The band at 1039 - 1076 cm^{-1} is attributed to the PO_4^{3-} absorption bands and the bands at 960 cm^{-1} and 568-600 cm^{-1} correspond to the symmetric P-O stretching vibration of PO_4^{3-} ion. The bands at 870 and 1453 cm^{-1} are attributed to the carbonate group (CO_3^{2-}). The characteristic peaks at 3436 cm^{-1} and 628 cm^{-1} are attributed to the stretching modes of hydroxyl groups (OH^-) in the hydroxyapatite [12, 13, 14].

The XRD diffractogram of the acrylic bone cement without sintered HA powder indicate amorphous structure. Fig. 9 shows the XRD results of the acrylic bone cement without sintered HA powder.

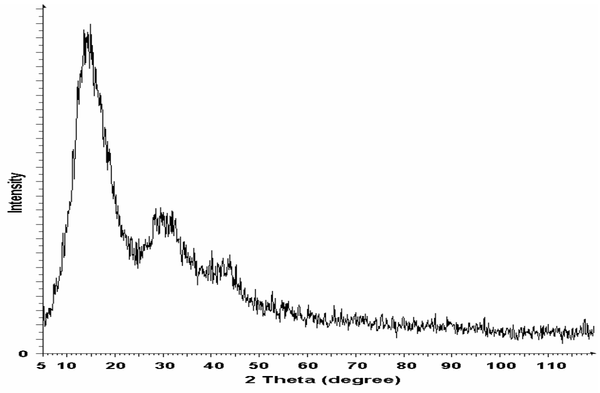

Fig. 9. XRD diffractogram of acrylic bone cement without HA powder.

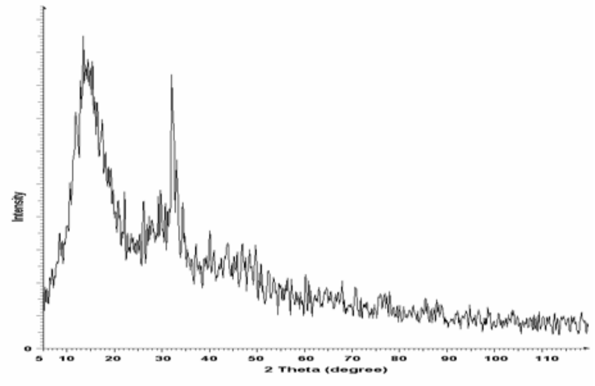

Fig. 10. XRD diffractogram of acrylic bone cement reinforced with HA powder.

According to the diffraction peaks of Fig. 10, the corresponding d spacings (Å) were determined: 7.61 (2Θ=11.62^0), and 2.91 (2Θ =30.76^0) correspond to PMMA, whereas the d spacings 3.43 (2Θ=25.8 ^{0}), 3.08 (2Θ= 28.9 ^{0}), 2.81 (2Θ=31.7 ^{0}), 2.62 (2Θ= 34.0 ^{0}), 2.25 (2Θ=39.9 ^{0}), 1.94 (2Θ=46.7 ^{0}), 1.88 (2Θ=48.1 ^{0}), 1.84 (2Θ=49.4 ^{0}) and 1.71 (2Θ =53.2^0), correspond to hexagonal system of HA powder [7, 8, 15].

According to SEM images presented in Fig. 11, the morphology of the acrylic bone cements is described as following. The PMMA beads (prepolymer) are distinguished in the acrylic bone cement, with the polymerized MMA connecting the beads, Fig. 11 (a). The cement without HA has more porous structure compared to reinforced with HA, Fig. 11(b). On the other hand, the reinforced cement contains two phases, indicating that HA is not mixed with PMMA remaining in a separate phase, however the voids decrease.

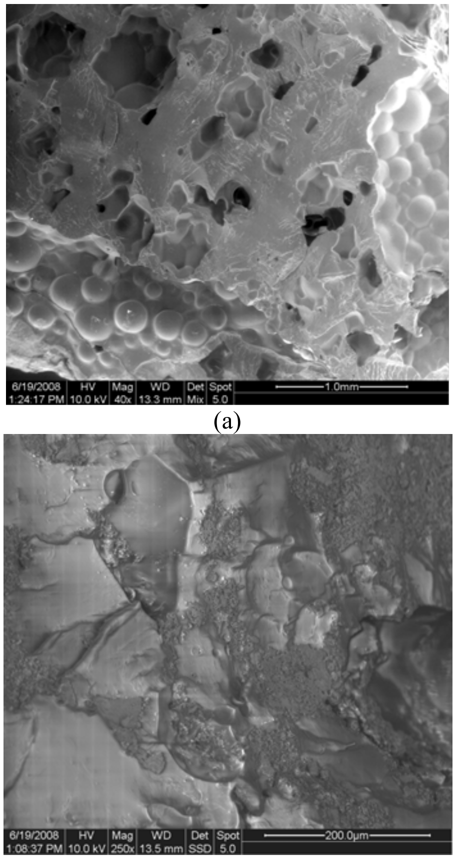

(a)

(b)

Fig.11. SEM images of (a) acrylic bone cement without HA and (b) reinforced with sintered HA powder.

According to Fig. 12, the limiting viscosity number of acrylic bone cement (without HA) is calculated as [n] = 0.7365 (100ml/g). The corresponding molecular weight is calculated from the Mark-Houwink-Sakurada equation, using the same values for the parameters K and a as that of PMMA beads and its value is : $\mathbf{M_w=4.6x10^5}$.

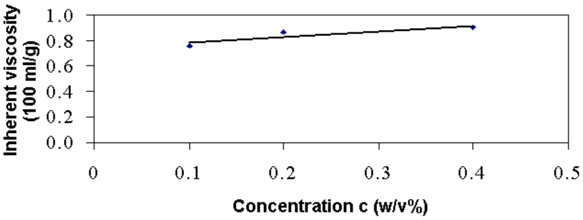

*Fig. 12. Plot of inherent viscosity versus the concentration **c** of acrylic bone cement (not reinforced with sintered HA powder).*

The molecular weight of both PMMA beads and bone cement is quite large. Specifically, the molecular weight of the acrylic bone cement (not reinforced with HA) was higher than that of the PMMA beads (prepolymer) due to the lower concentration of the initiator for the polymerization of MMA in the presence of PMMA prepolymer. Simultaneously, the reaction rate and the corresponding heat released are low. This is advantageous because the tissue damage during the surgery operation is diminished. In most cases in the literature, the molecular weight of the cement is higher than that of the PMMA prepolymer [16].

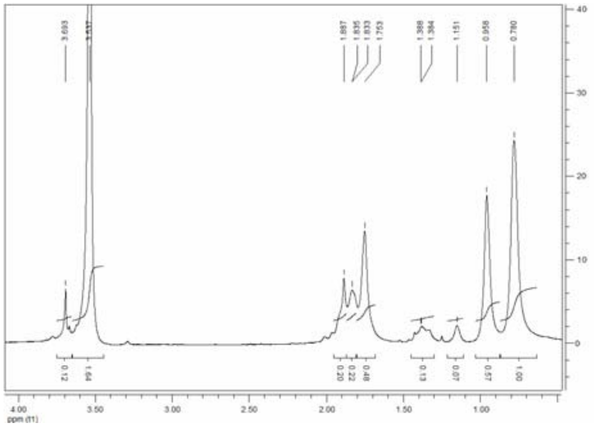

Fig. 13. ^{1}H-NMR spectrum of PMMA beads.

The ^{1}H NMR spectra of PMMA beads and acrylic bone cement without HA are presented in Figs. 13 and 14, respectively. According to literature [17], the three peaks in the region 0.2 – 1.2 ppm correspond to $–CH_3$, the three peaks between 1.4 – 2.0 ppm to $–CH_2$- and the two peaks between 3.4 – 3.8 ppm to $–OCH_3$. NMR spectroscopy is the only analytical means that provides quantitative data on tacticity [17]. The smallest unit representing relative configuration of the consecutive monomeric units (i.e. two) is termed a diad. For a vinyl polymer two types of diads should be considered: meso (m) and racemo (r). Thus, an isotactic polymer can be represented as: -mmmmmm- and a syndiotactic as: -rrrrrr-. The presence of more than one peak for certain hydrogen (e.g.-CH_3) indicates an atactic structure of both the polymers. However, segmental regularity is observed. The three groups of -CH_3, signals observed in Fig. 13 from 0.2 to 1.2 ppm are attributed to mm (isotactic), mr (heterotactic), and rr (syndiotactic) triads (i.e. three monomeric units). The two groups of -OCH_3, signals from 3.4 to 3.8 ppm are attributed to mm and rr triads [17].

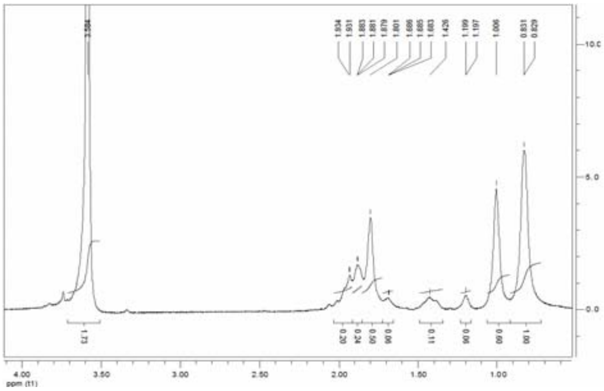

Fig. 14. ^{1}H-NMR spectrum of acrylic bone cement not reinforced with sintered HA powder.

The values of $[4*(mm)*(rr)/(mr)^2]$ is 0.86 for PMMA beads and 0.66 for acrylic bone cement. When the polymerization can be described by a Bernoullian statistics this value is unity. However, for the radically prepared PMMA, the values are clearly less than unity, indicating a deviation from Bernoullian statistics. It is remarkable that more deviation is observed for the acrylic bone cement compared to that of PMMA prepolymer.

Moreover, by comparing the spectra of the two materials, in the bone cement two set of peaks are exhibited in the region of 1.4 - 1.7 ppm which are not present in the spectra of PMMA prepolymer. These peaks can be attributed to methine hydrogen (i.e. –CH<) [17]. Thus, PMMA prepolymer can be considered as a linear polymer, whereas the bone cement as a branched polymer. Such a structure can be created by transfer reaction onto the macromolecules of PMMA prepolymer which are present from the beginning of the polymerization of MMA in the case of the acrylic bone cement. Transfer reactions taking place during the polymerization of MMA (in absence of PMMA prepolymer) lead to a decrease of the polymer molecular weight. However, these reactions taking place in the presence of PMMA prepolymer, i.e. in the backbone of the macromolecule, lead to the increase of the size of the macromolecule due to the branches created, and therefore to the increase of polymer molecular weight.

4. Conclusions

The PMMA beads obtained by suspension polymerization have spherical form with appropriate diameter between 17 and 250 μm. According to XRD, the sintered HA powder shows peaks of high intensity which belong to crystalline hydroxyapatite and peaks of low intensity attributed to b-tricalcium phosphate (TCP) and CaO, which are also biocompatible, probably derived from a small decomposition of HA powder during sintering.

The molecular weights of PMMA beads and bone cement without HA viscosimetrically determined were $2x10^5$ and $4.6x10^5$, respectively. The molecular weight of acrylic bone cement twice that of the PMMA prepolymer due to the low initiator concentration on the one hand and the creation of branches on the other hand.

According to the NMR spectra, the PMMA beads and the bone cement indicate that the polymers are atactic but there is a preference to the syndiotactic triads.

Acrylic bone cements reinforced with HA can be an advantageous solution for problems of bone filling as well as bone regeneration.

Acknowledgements

The authors would like to thank Prof. A. Vgenopoulos in the School of Mining Engineering and Metallurgy, NTUA, for the kindly helping for FTIR measurements and also Mr. Loukas Zoumpoulakis, Assistant Professor, in the School of Chemical Engineering, NTUA. The co-author (D. Baciu) wants to thank the Greek State Scholarship's Foundation (IKY) for its PhD-Scholarship.

References

[1] S. He, C. Scott, P. Higham, Mixing of acrylic bone cement: effect of oxygen on setting properties, Biomaterials **24**, 5045-5048 (2003).

[2] A. M. Moursi, A. V. Winnard, P. L. Winnard, J. J. Lannutti, R. R. Seghi, Enhanced osteoblast response to polymethylmethacrylate-hydroxyapatite composite, Biomaterials **23**, 133-144 (2002).

[3] S. Deb, L. Aiyathurai, J. A. Roether, Z. B. Luklinska, Development of high viscosity, two-paste bioactive bone cements, Biomaterials **26**, 3713-3718 (2005).

[4] S. Ramesh, C.Y. Tan, S.B. Bhaduri, W.D. Teng, I. Sopyan, Densification behaviour of nanocrystalline hydroxyapatite bioceramics, J. Materials Processing Technology **206**, 221-230 (2008).

[5] M. Ohgaki and K. Yamashita, Preparation of Polymethylmethacrylate-Reinforced Functionally Graded Hydroxyapatite Composites, J. Am. Ceram. Soc., **86** [8], 1440-42 (2003).

[6] X. Xiao, R. Liu, Q. Huang, Preparation and characterization of nano-hydroxyapatite/polymer composite scaffolds, J Mater. Sci: Mater. Med. **19**, 3429-3435 (2008).

[7] M. H. Fathi, A. Hanifi, Evaluation and characterization of nanostructure hydroxyapatite powder prepared by simple sol-gel method, Materials Letters **61**, 3978-3983 (2007).

[8] S. Ahmad, S. Ahmad and S. A. Agnihotry, Synthesis and characterization of *in situ* prepared poly (methyl methacrylate) nanocomposites, Bull. Mater. Sci., **30**, No. 1, pp. 31–35. February (2007) © Indian Academy of Sciences.

[9] C. Parra, Gema Gonzales, C. Albano, Synthesis and characterization of poly (methylmetacrylate) obtained by ultrasonic irradiation, e-Polymers, no. **025** (2005).

[10] S. Rajendran, T. Uma, Characterization of plasticized PMMA-$LiBF_4$ based solid polymer electrolytes, Bull. Mater. Sci., **23**, No. 1, p. 27-29, February (2000) ©Indian Academy of Sciences.

[11] J. Brandrup, E. H. Immergut and E. A. Grulke,Ed., Polymer Handbook, Fourth Edition VII/16 (1999).

[12] I. Bogdanoviciene, A. Beganskiene, K. Tonsuaadu, J. Glaser, H. Jurgen Meyer, A. Kareiva, Calcium hydroxyapatite (Ca_{10} $(PO_4)_6(OH)_2$, HA) ceramics prepared through aqueous sol-gel processing, Material Research Bulletin **41**, 1754-1762 (2006).

[13] H. M. Ledo, A. C. Thackray, I. P. Jones, P. M. Marquis, L. E. Macaskie, R. L. Sammons, Microstructure and composition of biosynthetically synthesised hydroxyapatite, J. Mater. Sci:Mater Med **19**, 3419-3427 (2008).

[14] G. Bezzi, G. Celotti, E. Landi, T. M. G. La Torretta, I. Sopyan, A. Tampieri, A novel sol-gel technique for hydroxyapatite preparation, Materials Chemistry and Physics **78**, 816-824 (2003).

[15] Y. Yuan, C. Liu, Y. Zhang, X. Shan, Sol-gel auto combustion synthesis of hydroxyapatite nanotubes array in porous alumina template, Materials Chemistry and Physics **112**, 275-280 (2008).

[16] S.C. Bayne, E.P. Lautenschlager, C.L. Compere, R. Wildes, Degree of polymerization of acrylic bone cement, J. Biomed. Mater. Res. **9**, 27 (1975).

[17] K. Hatada, T. Kitayama, NMR Spectroscopy of Polymers, Springer - Verlag Berlin Heidelberg, 76-87 (2004).

---

*Corresponding author: sinj@chemeng.ntua.gr